effects involving the orbital momentum as well as exchange effects,[20] it is difficult to comment considering the small values obtained.

Acknowledgments.—The authors thank Dr. Harry Gray for making available the magnetometer for low-temperature magnetic susceptibility measurements. In particular, thanks are expressed to Al Schweizer for his excellent instruction in the use of the magnetometer. Gratitude is also expressed to the National Science Foundation and the National Institutes of Health from which partial funding of the research was received.

(20) J. H. Van Vleck, "The Theory of Electric and Magnetic Susceptibilities," 1st ed, Oxford University Press, London, 1932, p 305.

CONTRIBUTION FROM THE DEPARTMENT OF CHEMISTRY, UNIVERSITY OF CALIFORNIA, IRVINE, IRVINE, CALIFORNIA 92664

Trigonal Prismatic–Octahedral Coordination. Complexes of Intermediate Geometry[1]

BY EVERLY B. FLEISCHER,* ALLEN E. GEBALA, DAVID R. SWIFT, AND PETER A. TASKER

Received May 3, 1972

The synthesis and characterization of the divalent metal complexes (Zn, Ni, Co, Fe, Mn) of the ligand 1,1,1-tris(pyridine-2-aldiminomethyl)ethane (py_3TPN) are described. X-Ray diffraction studies are reported for $[Zn(py_3TPN)](ClO_4)_2$, $[Fe(py_3TPN)](ClO_4)_2$, and *cis,cis*-1,3,5-tris(pyridine-2-aldimino)cyclohexanenickel(II) perchlorate, $[Ni(py_3tach)](ClO_4)_2$. The complex $[Zn(py_3TPN)](ClO_4)_2$ crystallizes in the centrosymmetric monoclinic space group $P2_1/a$ (c unique), with a = 19.993 (21) Å, b = 17.930 (20) Å, c = 15.320 (17) Å, γ = 150.64 (5)°, and ρ_{obsd} = 1.58, ρ_{calcd} = 1.59 g cm^{-3} for Z = 4; R_1 = 7.8% for 1614 reflections. It was determined, from precession photographs, that the Mn, Co, and Ni complexes are isomorphous with the Zn complex. The complex $[Fe(py_3TPN)](ClO_4)_2$ crystallizes in the noncentrosymmetric orthorhombic space group $P2_12_12_1$, with a = 11.827 (8), b = 21.266 (15), c = 10.667 (8) Å, and ρ_{obsd} = 1.59, ρ_{calcd} = 1.58 g cm^{-3} for Z = 4; R_1 = 6.7% for 1206 reflections. The complex $[Ni(py_3tach)](ClO_4)_2$ crystallizes in the noncentrosymmetric monoclinic space group Pc, with a = 15.470 (7) Å, b = 9.971 (5) Å, c = 20.503 (10) Å, β = 120.88 (2)°, and ρ_{obsd} = 1.62, ρ_{calcd} = 1.60 g cm^{-3} for Z = 4; R_1 = 7.5% for 1800 reflections. These complexes contain ligands that possess a trigonal axis, but are considerably distorted from octahedral geometry; angles of "twist" from such geometry are approximately 32° for $Zn(py_3TPN)^{2+}$, 28° for $Ni(py_3tach)^{2+}$, and 17° for $Fe(py_3TPN)^{2+}$. The structures of these and similar compounds are discussed in relation to their physical and spectroscopic properties and to the nature of the sexidentate ligand.

The first class of molecular complexes that was found to possess trigonal prismatic geometry were the metal tris(dithiolenes).[2] More recently, the tris(diselenetenes) have been found to exist in a similar geometry.[3] The earlier discovered metal sulfide compounds, with an infinite polymeric structure, also exist in a trigonal prismatic geometry.[4] These systems are possibly stabilized in the trigonal prismatic array by some type of S···S (Se) interaction.

For tris bidentate ligand complexes, such as the dithiolenes, the distortions from octahedral or trigonal prismatic coordination have been described[5] using two parameters (see Figure 1): (1) an angle, ϕ, describing the twist of the faces perpendicular to the threefold axis in these complexes and (2) the ratio of the distances, s/h, of the side of a triangular face to the height between the faces. These parameters are related by the ligand bite and metal–ligand bond lengths. Note, that for an octahedron ϕ = 60° and for a trigonal prism ϕ = 0°.

Trigonal prismatic complexes of a different type are the "clathro chelate" systems[6] in which the ligand geometry constrains the coordination geometry of the complex. A three-dimensional ligand system developed by Holm[7] (shown in Figure 2a) exists in a trigonal prismatic geometry for the nickel complex. It is surprising that even with such a rigid ligand, other effects can cause the ligand to rotate away from its preferred conformation and Fe(PccBF)$^+$ has an average ϕ of 21°. Another "clathro chelate" had previously been synthesized[8] from tris(dimethylglyoximato)-cobalt(III), which exists in a near trigonal prismatic geometry for the Co(II) complex (ϕ = 8.6°, Figure 2b), but in an intermediate geometry for Co(III) (ϕ = 31°).

Three systems of an open-trifurcated sexidentate type are represented in Figure 3 (a–c): (a) *cis,cis*-1,3,5-tris(pyridine-2-aldimino)cyclohexane,[9] for which the Zn(II) complex is known to possess near trigonal prismatic coordination (ϕ = 4.6°); (b) 1,1,1-tris(pyridine-2-aldiminomethyl)ethane, of which the Fe(II) complex has been prepared[10] and the very similar 1,1,1-

(1) Preliminary accounts of this work have appeared: E. B. Fleischer, A. E. Gebala, and P. A. Tasker, *J. Amer. Chem. Soc.*, **92**, 6365 (1970); E. B. Fleischer, A. E. Gebala, and D. R. Swift, *Chem. Commun.*, 1280 (1971).

(2) R. Eisenberg and J. A. Ibers, *J. Amer. Chem. Soc.*, **87**, 3776 (1965); A. E. Smith, G. N. Schrauzer, V. P. Mayweg, and W. Heinrich, *ibid.*, **87**, 5798 (1965); R. Eisenberg, E. I. Stiefel, R. C. Rosenberg, and H. B. Gray, *ibid.*, **88**, 2874 (1966); R. Eisenberg and J. A. Ibers, *Inorg. Chem.*, **5**, 411 (1966); R. Eisenberg and H. B. Gray, *ibid.*, **6**, 1844 (1967).

(3) C. G. Pierpont and R. Eisenberg, *J. Chem. Soc. A*, 2285 (1971).

(4) R. Dickinson and L. Pauling, *J. Amer. Chem. Soc.*, **45**, 1466 (1923).

(5) E. I. Stiefel and G. F. Brown, *Inorg. Chem.*, **11**, 434 (1972).

(6) D. H. Busch, *Rec. Chem. Progr.*, **25**, 107 (1964).

(7) J. E. Parks, B. E. Wagner, and R. H. Holm, *J. Amer. Chem. Soc.*, **92**, 3500 (1970); J. E. Parks, B. E. Wagner, and R. H. Holm, *Inorg. Chem.*, **10**, 2472 (1971); M. R. Churchill and A. H. Reis, Jr., *Chem. Commun.*, 879 (1970); M. R. Churchill and A. H. Reis, Jr., *ibid.*, 1307 (1971).

(8) D. R. Boston and N. J. Rose, *J. Amer. Chem. Soc.*, **90**, 6859 (1968); D. R. Boston and N. J. Rose, Abstracts, 157th National Meeting of the American Chemical Society, Minneapolis, Minn., April 1969, No. INOR-96; G. A. Zakrzewski, C. A. Ghilardi, and E. C. Lingafelter, *J. Amer. Chem. Soc.*, **93**, 4411 (1971).

(9) W. O. Gillum, J. C. Huffman, W. E. Streib, and R. A. D. Wentworth, *Chem. Commun.*, 843 (1969); W. O. Gillum, R. A. D. Wentworth, and R. F. Childers, *Inorg. Chem.*, **9**, 1825 (1970).

(10) D. A. Durham, F. A. Hart, and D. Shaw, *J. Inorg. Nucl. Chem.*, **29**, 509 (1967).

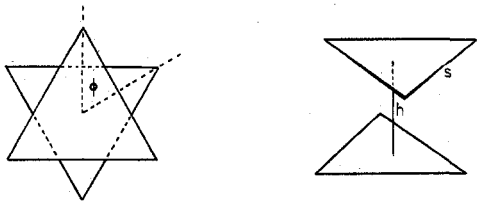

Figure 1.—Structural parameters used for characterization of trigonal prismatic *vs.* octahedral coordination for tris bidentate ligand complexes.

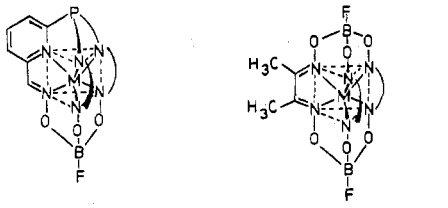

Figure 2.—Schematic representation of "clathro chelate" ligand complexes.

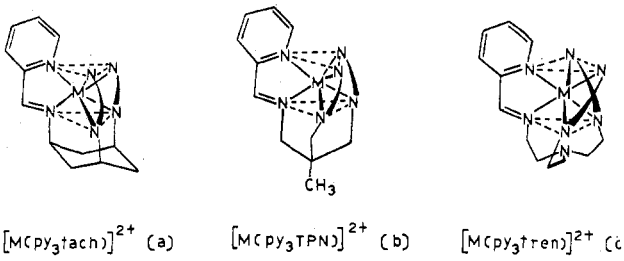

Figure 3.—Schematic drawings of open-trifurcated sexidentate ligand metal complexes.

tris(pyridine-2-aldiminomethyl)methaneiron(II) complex;[11] (c) tris(1-(2-pyridyl)-2-azabuten-4-yl)amine,[12] for which the Ni(II) and Fe(II) ($\phi = 54°$) are known to be nearly octahedral. This paper reports the synthesis and characterization of additional complexes of the type $M(py_3TPN)^{2+}$, X-ray structures of the zinc(II) and iron(II) perchlorate complexes, and the X-ray structure of the perchlorate salt of $Ni(py_3tach)^{2+}$. The purpose of our study was an attempt to experimentally determine, *via* X-ray diffraction, the geometries of some complexes of this type (that can attain geometries varying from octahedral to trigonal prismatic) and correlate them with various physical and spectroscopic properties. Factors such as ligand-field stabilization energies and ligand-imposed steric restraints were examined in order to arrive at possible predictive rules for the coordination geometry of these types of complexes.

Experimental Section

Preparation of Compounds.—1,1,1-Tris(aminomethyl)ethane (TPN) and *cis,cis*-1,3,5-triaminocyclohexane (tach) were prepared by the reduction of 1,1,1-tris(azidomethyl)ethane and *cis,cis*-1,3,5-triazidocyclohexane, respectively, in THF with $Li[AlH_4]$ and were purified by vacuum distillation.[13] Pyridine-2-carboxaldehyde was distilled under nitrogen prior to being used in the preparations of the metal complexes.

$[M(py_3TPN)](ClO_4)_2$.—TPN (1.17 g, 0.01 mol) and 3.21 g (0.03 mol) of pyridine-2-carboxaldehyde were dissolved in approximately 10 ml of anhydrous methanol and the resulting solution was refluxed gently under nitrogen for several minutes. A slight excess of the hexaaquometal perchlorate, dissolved in a minimum volume of anhydrous methanol, was added to the refluxing solution and refluxing was continued for about 2 min. After cooling, the crystalline material was filtered and recrystallized from either acetonitrile or an acetonitrile–ethanol mixture (50–50); the iron complex generally formed an oil that could be solidified by triturating with ethyl ether. The yield of the nickel complex was quite low while those for the other metals were good; the pure Cu complex could not be isolated using this procedure. Analytical data, recrystallization media, and physical appearance are presented in Table I.

$[Ni(py_3tach)](ClO_4)_2$.—This complex was prepared as previously published[9] and crystallized from water as orange prisms.

^1H nuclear magnetic resonance spectra were obtained for the d^6 low-spin Fe(II) and the diamagnetic Zn(II) complexes in D_3C-CN, using TMS as an internal standard, with Varian A60 and HA100 spectrometers. Ir spectra were taken, as Nujol and hexachlorobutadiene mulls, with a Beckman IR-10. Magnetic susceptibility data were obtained at room temperature with a Faraday balance calibrated with $Hg[Co(SCN)_4]$. Electronic spectra were recorded using a Cary 14 spectrometer for acetonitrile (spectral grade) solutions thermostatted at 25°.

Crystallographic Data

I. *cis,cis*-1,3,5-Tris(pyridine-2-aldimino)cyclohexanenickel(II) Perchlorate, $[Ni(py_3tach)](ClO_4)_2$.—Precession photographs using Zr-filtered Mo Kα radiation indicated that the crystals belonged to either space group $P2/c$ or Pc. Monoclinic unit cell parameters, obtained from the photographs, were refined using a least-squares method to yield the best fit between observed and calculated settings for χ, ϕ, and 2θ for 24 independent carefully centered reflections on a Picker four-angle diffractometer (take-off angle 1.0°, Mo Kα_1): $a = 15.470$ (7) Å, $b = 9.971$ (5) Å, $c = 20.503$ (10) Å, $\beta = 120.88$ (2)°, and $V = 2714.3$ Å^3. The measured (flotation, CCl_4–CH_2Br_2) and calculated ($Z = 4$) densities are 1.62 and 1.60 g cm^{-3}.

Intensity data were collected using the θ–2θ scan method employing Mo Kα radiation and a take-off angle of 1.5°. The diffracted beam was filtered with a Nb foil and the pulse-height analyzer set to accept about 90% of the Mo Kα peak. The peaks were scanned at 1°/min for a symmetric scan range of 2.0°, with allowances made for the Kα_1–Kα_2 split at higher 2θ values. Stationary-crystal, stationary-counter background counts of 10 sec were taken at each end of the scan range. Three reflections were monitored during data collection, (030), (700), and the (504), and were counted after every 100 reflections; no reduction in intensity of these monitors was observed during the course of data collection and none of the standards deviated by more than 1.8% from its average value. A total of 2796 reflections were collected.

The collected intensities were corrected for background, attenuators, Lorentz, polarization, and absorption (transmission factors ranging from 1.21 to 1.33). From counting statistics, 1800 of the 2796 collected reflections were considered $>3\sigma$. The data were placed on an approximate absolute scale with a Wilson plot and the program FAME[14] used to determine whether the distribution of electrons in the unit cell was centric or acentric. From the distribution of calculated normalized structure factors (E's), the crystal was indicated to belong to the noncentrosymmetric space group Pc and this was confirmed by the successful solution and refinement of the structure.

The structure was solved by the straightforward application of Patterson, Fourier, and least-squares techniques; the only problems encountered arising from the large number of independent nonhydrogen atoms (82) in the unit cell. Scattering

(11) F. P. Dwyer, N. S. Gill, E. C. Gyarfas, and F. Lions, *J. Amer. Chem. Soc.*, **79**, 1269 (1957).

(12) L. J. Wilson and N. J. Rose, *ibid.*, **90**, 6041 (1968); M. F. Bailey and E. C. Lingafelter, Abstracts, 156th National Meeting of the American Chemical Society, Atlantic City, N. J., Sept 1968, No. INOR-28; C. Meali and E. C. Lingafelter, *Chem. Commun.*, 885 (1970).

(13) E. B. Fleischer, A. E. Gebala, P. A. Tasker, and A. Levy, *J. Org. Chem.*, **36**, 3042 (1971).

(14) R. B. K. Dewar, Dissertation, "The Use of Computers in the X-Ray Phase Problem," The University of Chicago, 1968.

TABLE I

ANALYTICAL DATA[a] FOR $[M(py_3TPN)](ClO_4)_2$ COMPLEXES

Complex	% calcd C	% calcd H	% calcd N	% found C	% found H	% found N	Solvent	Color
$[Mn(py_3TPN)](ClO_4)_2$	43.28	3.79	13.17	43.24	3.77	13.20	ACN–EtOH	Light orange
$[Fe(py_3TPN)](ClO_4)_2$	43.22	3.78	13.15	43.08	3.77	13.06	ACN–EtOH	Dark violet
$[Co(py_3TPN)](ClO_4)_2$	43.01	3.77	13.08	43.85	3.87	13.38	ACN–EtOH	Red-orange
$[Ni(py_3TPN)](ClO_4)_2$	43.02	3.77	13.09	43.18	3.88	13.29	ACN	Red-orange
$[Zn(py_3TPN)](ClO_4)_2$	42.58	3.73	12.95	42.76	3.73	13.02	ACN	Colorless

[a] Analyses performed by Micro-Tech Laboratories, Inc., Skokie, Ill.

factors were taken from ref 15 and the effects of anomalous dispersion for Ni and Cl included in their contributions to the calculated structure factors, with values of $\Delta f'$ and $\Delta f''$ taken from ref 16. Anisotropic temperature factors, of the form $\exp[-(\beta_{11}h^2 + \beta_{22}k^2 + \beta_{33}l^2 + 2\beta_{12}hk + 2\beta_{13}hl + 2\beta_{23}kl)]$, were used for Ni and for O and Cl of three of the four perchlorate groups (the fourth being badly disordered) in the final cycles of refinement. Refinement was carried to a conventional R factor of 0.075; $R = \Sigma||F_o| - |F_c||/\Sigma|F_o|$.

The final atom positional and thermal parameters, along with their estimated standard deviations, are presented in Table II. Bond distances and bond angles for the coordination sphere are listed in Table III. A table of observed and calculated structure factors is available.[17]

II. 1,1,1-Tris(pyridine-2-aldiminomethyl)ethanezinc(II) Perchlorate, $[Zn(py_3TPN)](ClO_4)_2$.—Precession photographs obtained with Ni-filtered Cu Kα radiation indicated the crystal belonged to the monoclinic space group $P2_1/c$; this was subsequently changed to $P2_1/a$ with c unique due to the special geometry of the instrument used for data collection. Precession photographs of the Ni(II), Co(II), and Mn(II) complexes indicated that these crystals were isomorphous, and probably close in structural detail, with $[Zn(py_3TPN)](ClO_4)_2$. A least-squares refinement of the cell constants obtained from photographs of measured and calculated settings of χ, ϕ, and 2θ for 26 independent reflections centered on a Picker four-angle automatic diffractometer (take-off angle 1.0°, Mo Kα_1) resulted in cell constants of a = 19.993 (21) Å, b = 17.930 (20) Å, c = 15.320 (18) Å, γ = 150.64 (5)°, and V = 2692.5 Å^3. A measured density of 1.58 g cm^{-3} (flotation, CCl_4–CH_2Br_2) compares well with a calculated density (Z = 4) of 1.59 g cm^3.

A total of 5150 reflections were collected using a Pailred automatic diffractometer employing graphite monochromated Mo Kα radiation on a crystal aligned about the c (unique) axis (hkl; l = 0–16). An ω scan range of 4° and scan rate of 5°/min was used for data collection and backgrounds were counted for 10 sec at each end of the scan range. After every layer collected, the ($\bar{8}50$) reflection was monitared to check crystal and instrument stability; no significant decomposition was observed during data collection and the standard was constant to within ±3%.

After averaging of duplicate peaks and rejecting those for which $I \leq 3\sigma$ there remained 1614 intensities that were considered observed and were used in the solution and refinement of the structure. The measured intensities were corrected for background, Lorentz, and polarization; no absorption correction was applied to the data.

The structure was solved by Patterson, Fourier, and least-squares techniques and no difficulties were encounted. Scattering factors were taken from ref 15 and the effects of anomalous dispersion, $\Delta f'$ and $\Delta f''$, for Zn and Cl[16] were included in the calculated structure factors. In the final least-squares cycles of refinement, anisotropic temperature factors were used (of the form used in the refinement of the Ni structure) for Zn, N, and Cl and O of one of the two perchlorate groups; attempts to construct a suitable disordered model for the second perchlorate group met with repeated failure and isotropic thermal parameters were used in the refinement. Nonmethyl hydrogen atoms were placed in calculated positions and assigned isotropic thermal parameters of the adjacent carbon atoms for the final cycles of refinement. Positional and thermal parameters for the hydrogen atoms were not varied in any least-squares cycle, but were recalculated before the next cycle of refinement. Prior to the incorporation of the hydrogen atoms in the refinement, a difference map was examined and showed electron density at the calculated positions. Final conventional R factor = 0.078.

A list of atomic positional and thermal parameters, with estimated standard deviations, is given in Table IV and a list of bond distances and angles for the coordination sphere is given in Table III. A table of observed and calculated structure factors is available.[17]

III. 1,1,1-Tris(pyridine-2-aldiminomethyl)ethaneiron(II) Perchlorate, $[Fe(py_3TPN)](ClO_4)_2$.—Precession photographs taken with Ni-filtered Cu Kα radiation showed that the crystal belonged to space group $P2_12_12_1$. Approximate cell constants obtained from the photographs were refined by a least-squares method using 45 θ_{hkl}'s measured with a General Electric single-crystal orienter employing Cu Kα radiation: a = 11.827 (8) Å, b = 21.266 (15) Å, c = 10.667 (8) Å, and V = 2682.9 Å^3. The measured (flotation, $CHCl_3$–CH_2Br_2) and calculated (Z = 4) densities are 1.59 and 1.58 g cm^{-3}, respectively.

Intensity data were collected on a Pailred automatic diffractometer with a crystal mounted along the c axis (l = 0–12); a total of 5168 intensities were measured from two quadrants, hkl and $\bar{h}kl$. An ω scan rate of 2.5°/min was used for data collection and a scan width of 4.0°, with backgrounds of 20 sec at each end of the scan, was used. After each layer was collected, the (041) reflection was checked to monitor crystal and instrument stability; no decomposition was noted during data collection and the maximum deviation from the average of the standards was within ±4%.

The data were corrected for background, Lorentz, and polarization, but no absorption correction was applied to the data. After averaging the data from the two quadrants and rejecting intensities for which the ratio of the backgrounds exceeded 1.5 and those with counting errors of >0.5, 1206 reflections remained and were considered observed and used in the solution and refinement of the structure. The counting error used was $\Delta I/I = (T + t^2B)^{1/2}/(T - tB)$, where B is the sum of the background counts from both ends of the scan, T is the total counts of the peak (ω scan), and $t = t_s/t_b$, the ratio of times for the scan and background. For related intensities, the average difference is 3.5%.

Patterson, Fourier, and least-squares techniques were used for the solution and refinement of the structure and no difficulties were encountered. Scattering factors were taken from ref 15. Anisotropic temperature factors (of the same form as used in the refinement of the Ni structure) for Fe, N, Cl, and O were used in the final least-squares cycles. Nonmethyl hydrogen atoms were placed in calculated positions, with isotropic temperature factors of the attached carbon atoms assigned, and included in the final cycles of refinement; these parameters were not varied in any given cycle, but they were recalculated before the next cycle of least-squares refinement. A difference map, prior to inclusion of the hydrogen atoms, showed electron density at these calculated positions. The highest peaks in the difference map were at hydrogen atom positions and this precludes the presence of water of crystallization, as was reported for 1,1,1-tris(pyridine-2-aldiminomethyl)methaneiron(II) perchlorate;[11] the chemical analysis of $[Fe(py_3TPN)](ClO_4)_2$ also supports the lack of water of crystallization (see Table I). A final conventional R factor of 6.7% was attained.

A list of atomic positions and temperature factors is given in Table V, with estimated standard deviations, and a list of bond distances and angles for the coordination sphere is given in Table III. A table of observed and calculated structure factors

(15) "International Tables for X-Ray Crystallography," Vol. 3, Kynoch Press, Birmingham, England, 1962, Table 3.3.1A.

(16) Reference 15, Table 3.3.2C.

(17) A listing of structure factor amplitudes will appear following these pages in the microfilm edition of this volume of this journal. Single copies may be obtained from the Business Operations Office, Books and Journals Division, American Chemical Society, 1155 Sixteenth St., N.W., Washington, D. C. 20036, by referring to code number INORG-72-2775. Remit check or money order for $3.00 for photocopy or $2.00 for microfiche.

TABLE II

ATOMIC PARAMETERS AND ANISOTROPIC TEMPERATURE FACTORS FOR THE STRUCTURE [Ni(py$_3$tach)](ClO$_4$)$_2$[b]

Atomic Parameters

Atom	x	y	z	B
Ni(1)	−0.0800 (2)	0.152 (3)	0.2600 (2)	*a*
Ni(2)	0.3688 (2)	0.2421 (3)	0.2050 (2)	*a*
Cl(1)	−0.3179 (8)	0.1448 (11)	−0.1511 (6)	*a*
Cl(2)	0.0868 (7)	0.2191 (10)	−0.4182 (5)	*a*
Cl(3)	0.3135 (8)	0.4085 (11)	−0.0491 (6)	*a*
Cl(4)	−0.3211 (10)	0.3297 (13)	−0.4308 (7)	8.6 (9)
O(11)	−0.236 (3)	0.191 (4)	−0.082 (2)	*a*
O(12)	−0.408 (3)	0.184 (4)	−0.161 (2)	*a*
O(13)	−0.327 (3)	0.003 (4)	−0.154 (2)	*a*
O(14)	−0.308 (3)	0.194 (4)	−0.212 (2)	*a*
O(21)	0.086 (2)	0.131 (3)	−0.472 (2)	*a*
O(22)	0.178 (2)	0.211 (3)	−0.349 (2)	*a*
O(23)	0.007 (2)	0.174 (3)	−0.407 (2)	*a*
O(24)	0.067 (2)	0.352 (3)	−0.438 (2)	*a*
O(31)	0.325 (2)	0.407 (3)	−0.112 (2)	*a*
O(32)	0.383 (3)	0.329 (4)	0.010 (2)	*a*
O(33)	0.214 (3)	0.374 (4)	−0.069 (2)	*a*
O(34)	0.329 (3)	0.541 (4)	−0.022 (2)	*a*
O(41)	−0.331 (3)	0.196 (4)	−0.393 (2)	12.5 (1)
O(42)	−0.254 (3)	0.391 (5)	−0.366 (3)	20.4 (1)
O(43)	−0.332 (4)	0.429 (6)	−0.491 (3)	26.9 (1)
O(44)	−0.423 (2)	0.372 (3)	−0.456 (2)	21.6 (1)
N(11)	−0.087 (1)	−0.016 (2)	0.205 (1)	*a*
N(12)	−0.092 (2)	0.023 (2)	0.337 (1)	*a*
N(13)	0.077 (2)	0.116 (2)	0.330 (1)	*a*
N(14)	−0.220 (2)	0.178 (2)	0.162 (1)	*a*
N(15)	−0.115 (1)	0.289 (2)	0.324 (1)	*a*
N(16)	−0.017 (1)	0.307 (2)	0.231 (1)	*a*
C(11)	−0.028 (2)	−0.141 (3)	0.238 (2)	4.3 (6)
C(12)	−0.073 (2)	−0.195 (3)	0.284 (1)	4.8 (5)
C(13)	−0.040 (2)	−0.103 (3)	0.361 (1)	4.8 (6)
C(14)	0.0712 (2)	−0.086 (3)	0.409 (1)	4.4 (6)
C(15)	0.118 (2)	−0.025 (3)	0.360 (1)	5.2 (8)
C(16)	0.084 (2)	−0.116 (3)	0.283 (1)	4.4 (7)
C(141)	−0.292 (2)	0.284 (3)	0.142 (2)	6.0 (8)
C(142)	−0.371 (2)	0.284 (3)	0.066 (2)	6.2 (9)
C(143)	−0.379 (2)	0.197 (3)	0.016 (2)	6.5 (8)
C(144)	−0.312 (2)	0.095 (3)	0.029 (2)	5.8 (6)
C(145)	−0.232 (2)	0.089 (3)	0.105 (2)	4.6 (6)
C(146)	−0.163 (2)	0.020 (3)	0.135 (2)	4.6 (7)
C(151)	−0.128 (2)	0.418 (3)	0.316 (2)	4.6 (6)
C(152)	−0.156 (2)	0.498 (3)	0.362 (2)	4.4 (8)
C(153)	−0.176 (2)	0.433 (3)	0.409 (2)	5.0 (7)
C(154)	−0.169 (2)	0.293 (3)	0.415 (1)	4.3 (6)
C(155)	−0.136 (2)	0.234 (3)	0.374 (1)	3.8 (6)
C(156)	−0.116 (2)	0.078 (3)	0.383 (1)	4.4 (7)
C(161)	−0.064 (2)	0.403 (3)	0.175 (1)	4.1 (9)
C(162)	−0.005 (2)	0.519 (3)	0.170 (2)	5.8 (8)
C(163)	0.092 (2)	0.515 (3)	0.216 (2)	6.0 (7)
C(164)	0.148 (2)	0.420 (3)	0.275 (2)	6.0 (7)
C(165)	0.086 (2)	0.308 (3)	0.279 (2)	4.9 (6)
C(166)	0.135 (2)	0.199 (3)	0.326 (2)	*a*
N(21)	0.335 (1)	0.411 (2)	0.149 (1)	*a*
N(22)	0.415 (1)	0.363 (2)	0.301 (1)	*a*
N(23)	0.514 (1)	0.269 (2)	0.233 (1)	*a*
N(24)	0.211 (1)	0.237 (2)	0.143 (1)	*a*
N(25)	0.378 (1)	0.105 (2)	0.289 (1)	*a*
N(26)	0.383 (1)	0.088 (2)	0.143 (1)	*a*
C(21)	0.405 (2)	0.536 (2)	0.174 (1)	4.5 (6)
C(22)	0.409 (2)	0.583 (3)	0.242 (1)	4.6 (6)
C(23)	0.469 (2)	0.491 (3)	0.313 (1)	5.4 (6)
C(24)	0.571 (2)	0.458 (3)	0.325 (1)	5.8 (6)
C(25)	0.568 (2)	0.398 (3)	0.254 (1)	4.2 (6)
C(26)	0.511 (2)	0.496 (2)	0.185 (1)	5.1 (6)
C(241)	0.144 (2)	0.144 (3)	0.146 (1)	4.7 (6)
C(242)	0.044 (2)	0.161 (2)	0.094 (1)	4.3 (5)
C(243)	0.003 (2)	0.256 (3)	0.041 (1)	4.8 (6)
C(244)	0.068 (2)	0.350 (3)	0.036 (1)	4.9 (6)
C(245)	0.174 (2)	0.331 (2)	0.092 (1)	2.5 (5)
C(246)	0.237 (2)	0.437 (2)	0.096 (1)	4.1 (5)
C(251)	0.359 (2)	−0.026 (3)	0.280 (1)	4.4 (6)
C(252)	0.360 (2)	−0.112 (3)	0.336 (2)	7.4 (7)
C(253)	0.388 (2)	−0.045 (3)	0.409 (1)	5.2 (6)
C(254)	0.408 (2)	0.083 (3)	0.414 (2)	6.1 (7)

TABLE II (*Continued*)

Atom	x	y	z	B
C(255)	0.401 (2)	0.162 (2)	0.356 (1)	3.9 (5)
C(256)	0.429 (2)	0.305 (2)	0.363 (1)	4.4 (6)
C(261)	0.314 (2)	−0.001 (3)	0.099 (1)	4.2 (5)
C(262)	0.338 (2)	−0.125 (2)	0.070 (1)	4.7 (6)
C(263)	0.432 (2)	−0.147 (3)	0.092 (1)	4.7 (6)
C(264)	0.507 (2)	−0.054 (3)	0.138 (1)	5.9 (6)
C(265)	0.479 (2)	0.068 (2)	0.163 (1)	3.2 (5)
C(266)	0.549 (2)	0.179 (3)	0.216 (1)	8.2 (6)

Anisotropic Temperature Factors ($\times 10^4$)

Atom	β_{11}	β_{22}	β_{33}	β_{12}	β_{13}	β_{23}
Ni(1)	49 (2)	89 (3)	31 (2)	−1 (2)	20 (4)	2 (1)
Ni(2)	45 (2)	98 (4)	26 (1)	−3 (3)	16 (1)	0 (2)
Cl(1)	54 (2)	155 (3)	59 (2)	26 (3)	25 (2)	1 (2)
Cl(2)	60 (3)	93 (2)	43 (2)	22 (3)	20 (1)	3 (2)
Cl(3)	81 (2)	149 (3)	49 (3)	1 (3)	34 (2)	−10 (3)
O(11)	90 (13)	358 (14)	63 (3)	−68 (3)	−10 (3)	−50 (3)
O(12)	92 (13)	291 (14)	114 (3)	35 (3)	72 (2)	36 (3)
O(13)	177 (13)	63 (13)	129 (13)	70 (2)	53 (3)	0 (3)
O(14)	159 (12)	513 (13)	62 (13)	−89 (3)	46 (2)	0 (3)
O(21)	108 (13)	253 (14)	73 (12)	42 (13)	33 (13)	48 (3)
O(22)	87 (13)	299 (13)	41 (13)	67 (12)	−18 (13)	−22 (13)
O(23)	107 (13)	235 (15)	84 (13)	−45 (13)	63 (13)	6 (13)
O(24)	91 (13)	149 (14)	89 (12)	−48 (13)	27 (12)	−11 (14)
O(31)	138 (14)	302 (15)	83 (12)	117 (13)	77 (12)	46 (13)
O(32)	167 (13)	324 (14)	63 (13)	67 (13)	41 (12)	31 (14)
O(33)	157 (14)	343 (15)	104 (12)	−33 (13)	70 (12)	4 (14)
O(34)	156 (5)	285 (5)	118 (3)	0 (3)	71 (4)	−32 (1)
N(11)	54 (13)	90 (13)	30 (12)	0 (12)	27 (13)	−3 (12)
N(12)	45 (14)	125 (15)	38 (13)	−13 (13)	23 (13)	7 (12)
N(13)	94 (15)	79 (13)	54 (12)	29 (13)	44 (13)	12 (13)
N(14)	68 (14)	127 (13)	50 (13)	−24 (13)	36 (13)	22 (13)
N(15)	49 (14)	93 (13)	34 (13)	7 (14)	9 (12)	4 (14)
N(16)	33 (14)	76 (14)	34 (12)	−11 (14)	21 (13)	4 (13)
N(21)	61 (14)	72 (26)	35 (8)	−22 (16)	21 (9)	−19 (12)
N(22)	70 (16)	94 (30)	46 (9)	−4 (18)	36 (10)	−11 (14)
N(23)	66 (14)	91 (28)	56 (8)	−40 (20)	38 (9)	−31 (13)
N(24)	66 (13)	116 (26)	26 (7)	9 (17)	28 (8)	−8 (12)
N(25)	38 (15)	106 (30)	29 (9)	18 (16)	20 (9)	−3 (12)
N(26)	45 (12)	81 (23)	20 (7)	−16 (15)	15 (8)	−6 (11)

[a] See anisotropic temperature factors. [b] Numbers in parentheses in this and subsequent Tables are the estimated standard deviations in the least significant figures as determined by the least-squares treatment.

TABLE III
SOME BOND DISTANCES (Å) AND ANGLES (DEG) IN THE COORDINATION SPHERE OF THE COMPLEXES

Nickel Complex

Ni(1)–N(11)	2.00 (3)	Ni(2)–N(21)	1.96 (4)
Ni(1)–N(12)	2.12 (4)	Ni(2)–N(22)	2.10 (4)
Ni(1)–N(13)	2.13 (4)	Ni(2)–N(23)	2.04 (4)
Ni(1)–N(14)	2.08 (4)	Ni(2)–N(24)	2.10 (4)
Ni(1)–N(15)	2.15 (4)	Ni(2)–N(25)	2.13 (4)
Ni(1)–N(16)	2.07 (4)	Ni(2)–N(26)	2.08 (4)
N(11)–Ni(1)–N(12)	85 (2)	N(21)–Ni(2)–N(22)	85 (2)
N(11)–Ni(1)–N(13)	87 (2)	N(21)–Ni(2)–N(23)	88 (2)
N(14)–Ni(1)–N(15)	93 (2)	N(24)–Ni(2)–N(25)	93 (2)
N(14)–Ni(1)–N(16)	93 (2)	N(24)–Ni(2)–N(26)	94 (2)

Iron Complex		Zinc Complex	
Fe–N(1)	1.89 (2)	Zn–N(1)	2.11 (1)
Fe–N(2)	1.99 (2)	Zn–N(2)	2.18 (1)
Fe–N(3)	1.94 (2)	Zn–N(3)	2.16 (1)
Fe–N(4)	2.01 (1)	Zn–N(4)	2.15 (1)
Fe–N(5)	1.90 (1)	Zn–N(5)	2.17 (1)
Fe–N(6)	2.01 (2)	Zn–N(6)	2.15 (1)
N(1)–Fe–N(2)	82 (1)	N(1)–Zn–N(2)	76 (1)
N(1)–Fe–N(3)	86 (1)	N(1)–Zn–N(3)	82 (1)
N(1)–Fe–N(4)	96 (1)	N(1)–Zn–N(4)	82 (1)
N(1)–Fe–N(5)	88 (1)	N(1)–Zn–N(5)	110 (1)
N(1)–Fe–N(6)	166 (1)	N(1)–Zn–N(6)	153 (1)
N(5)–Fe–N(2)	101 (1)	N(5)–Zn–N(2)	96 (1)
N(5)–Fe–N(3)	87 (1)	N(5)–Zn–N(3)	76 (1)
N(5)–Fe–N(4)	166 (1)	N(5)–Zn–N(4)	151 (1)
N(5)–Fe–N(6)	80 (1)	N(5)–Zn–N(6)	97 (1)

is available.[17] Computer programs used in this study are listed in ref 18.

Discussion

The independently determined structures for the two $Ni(py_3tach)^{2+}$ ions of the asymmetric unit were shown to be the same within the limits of errors of the determination, and one of the cations is illustrated in Figure 4. The structure of $Zn(py_3TPN)^{2+}$ is given in Figure 5 and a stereo diagram is shown in Figure 6, while the analogous drawings for $Fe(py_3TPN)^{2+}$ are shown in Figures 7 and 8, respectively.

There are no unusual features revealed by bond distances of the ligands in each of the three determined structures. For $[Ni(py_3tach)](ClO_4)_2$ the 12 C–C bonds in the two cyclohexane rings of the asymmetric unit average to 1.56 Å. The errors estimated from the least-squares analysis are ±0.04 Å for these bonds. In the more accurately determined structures $[Zn(py_3TPN)](ClO_4)_2$ and $[Fe(py_3TPN)](ClO_4)_2$, some of the average bond lengths are as follows: $C_{sp^3}–C_{sp^3}$ = 1.549 ± 0.038 Å and $C_{sp^2}–C_{sp^2}$ = 1.38 ± 0.028 Å. The standard deviations of the average of chemically

(18) Data processing: Pailred data, PST and PLR (Dewar); Picker data, PICKOUT (Doedens and Ibers), PICK (Ibers); absorption, GONO (Hamilton); Fourier, FORDAP (Zalkin); least-squares refinement, UCIGLS local version of ORFLS (Busing, Martin, and Levy); bond parameters, ORFFE (Busing, Martin, and Levy); figures, ORTEP (Johnson).

TABLE IV
ATOMIC PARAMETERS AND ANISOTROPIC TEMPERATURE FACTORS FOR THE STRUCTURE $[Zn^{II}(py_3TPN)](ClO_4)_2$

Atomic Parameters

Atom	x	y	z	B
Zn	0.3731 (2)	0.0864 (2)	0.1612 (1)	[a]
Cl(1)	0.2746 (6)	−0.2752 (6)	0.1577 (4)	[a]
Cl(2)	0.3485 (5)	−0.2895 (6)	0.4715 (3)	[a]
O(11)	0.2631 (1)	0.383 (1)	−0.367 (1)	[a]
O(12)	0.169 (2)	0.174 (2)	−0.401 (1)	[a]
O(13)	0.312 (2)	0.326 (2)	−0.284 (1)	[a]
O(14)	0.090 (3)	0.156 (3)	−0.289 (2)	[a]
O(21)	0.108 (1)	0.297 (2)	−0.097 (1)	6.3 (6)
O(22)	0.049 (2)	0.170 (2)	0.029 (1)	11.2 (7)
O(23)	0.195 (3)	0.266 (3)	−0.064 (2)	14.3 (8)
O(24)	0.252 (3)	0.424 (3)	0.018 (2)	15.7 (7)
N(1)	0.445 (1)	0.067 (1)	0.238 (1)	[a]
N(2)	0.219 (1)	−0.075 (1)	0.263 (1)	[a]
N(3)	0.518 (1)	0.181 (1)	0.069 (1)	[a]
N(4)	0.248 (1)	−0.076 (1)	0.056 (1)	[a]
N(5)	0.559 (1)	0.319 (1)	0.209 (1)	[a]
N(6)	0.343 (1)	0.174 (1)	0.135 (1)	[a]
C(1)	0.832 (2)	0.434 (2)	0.202 (1)	4.8 (4)
C(2)	0.681 (2)	0.320 (2)	0.189 (1)	3.3 (3)
C(3)	0.581 (2)	0.164 (2)	0.226 (1)	4.1 (3)
C(4)	0.372 (2)	−0.024 (2)	0.301 (1)	4.0 (3)
C(5)	0.245 (2)	−0.106 (2)	0.315 (1)	3.3 (3)
C(6)	0.155 (2)	−0.215 (2)	0.384 (1)	4.9 (4)
C(7)	0.046 (2)	−0.277 (2)	0.398 (1)	5.5 (4)
C(8)	0.013 (2)	−0.250 (2)	0.345 (1)	5.1 (4)
C(9)	0.108 (2)	−0.142 (2)	0.278 (1)	3.7 (3)
C(10)	0.663 (2)	0.314 (2)	0.089 (1)	3.9 (4)
C(11)	0.463 (2)	0.092 (2)	0.008 (1)	3.6 (3)
C(12)	0.317 (2)	−0.045 (2)	−0.006 (1)	2.7 (3)
C(13)	0.253 (2)	−0.137 (2)	−0.079 (1)	4.8 (4)
C(14)	0.114 (2)	−0.264 (2)	−0.087 (1)	5.8 (5)
C(15)	0.041 (2)	−0.301 (2)	−0.025 (1)	5.0 (4)
C(16)	0.110 (2)	−0.205 (2)	0.045 (1)	4.1 (4)
C(17)	0.676 (2)	0.387 (2)	0.238 (1)	3.5 (3)
C(18)	0.572 (2)	0.399 (2)	0.190 (1)	3.4 (3)
C(19)	0.452 (1)	0.322 (2)	0.155 (1)	2.5 (2)
C(20)	0.455 (2)	0.400 (2)	0.142 (1)	4.5 (4)
C(21)	0.340 (2)	0.324 (2)	0.104 (1)	5.0 (4)
C(22)	0.229 (2)	0.173 (2)	0.087 (1)	4.3 (4)
C(23)	0.234 (2)	0.102 (2)	0.103 (1)	3.8 (3)

Anisotropic Temperature Factors ($\times 10^4$)

Atom	β_{11}	β_{22}	β_{33}	β_{12}	β_{13}	β_{23}
Zn	54 (2)	72 (2)	37 (4)	51 (2)	0 (1)	2 (1)
Cl(1)	214 (8)	168 (13)	61 (12)	167 (8)	55 (15)	41 (6)
O(11)	168 (8)	135 (16)	85 (14)	127 (7)	14 (6)	16 (8)
O(12)	382 (14)	431 (11)	105 (12)	387 (9)	−121 (8)	−135 (9)
O(13)	301 (12)	252 (13)	137 (11)	241 (15)	−138 (9)	−96 (5)
O(14)	419 (16)	372 (12)	176 (11)	348 (13)	93 (10)	114 (7)
N(1)	61 (15)	68 (18)	42 (7)	51 (16)	0 (8)	2 (9)
N(2)	69 (14)	86 (20)	38 (6)	63 (17)	3 (8)	−7 (9)
N(3)	38 (13)	82 (19)	41 (6)	45 (15)	7 (8)	11 (9)
N(4)	71 (16)	99 (21)	40 (7)	72 (18)	−13 (8)	−10 (9)
N(5)	72 (16)	88 (19)	35 (6)	68 (16)	−8 (8)	−12 (9)
N(6)	88 (17)	109 (21)	38 (7)	89 (19)	5 (8)	3 (9)

[a] See anisotropic temperature factors.

equivalent bonds are slightly larger than the estimated standard deviations of ≃0.03 Å in individual C–C bonds.

The extent to which these complexes deviate from the idealized coordination geometries of a trigonal prism or an octahedron is compared using the trigonal twist parameter $\bar{\phi}$ in Table VI. These $\bar{\phi}$ values are obtained by projecting the aldimino nitrogen triangular face onto the pyridine nitrogen triangular face and averaging the three resulting ϕ's (see Figure 1a). The mean deviation from this average is less than 2° for the complexes included in Table VI.

The two complexes $Ni(py_3tach)^{2+}$ and $Zn(py_3TPN)^{2+}$ are almost halfway between the two idealized geometries ($\phi \simeq 32$ and 28°) whereas the $Fe(py_3TPN)^{2+}$ ion is closer to an octahedron ($\phi = 43°$). Other related compounds are included in Table VI and sufficient data are now available to allow the comparison of several important pairs of complexes containing the same metal ion. The zinc complex, $Zn(py_3tach)^{2+}$, studied by Wentworth, *et al.*,[9] shows a coordination geometry very close to a trigonal prism, which contrasts with the intermediate geometry found in this work for $Zn(py_3TPN)^{2+}$. Similarly $Ni(PccBF)^{+}$ is almost perfectly trigonal prismatic whereas $Ni(py_3tach)^{2+}$, and probably $Ni(py_3TPN)^{2+}$, has intermediate geometry. Both $Fe(PccBF)^{+}$ and $Fe(py_3TPN)^{2+}$ show marked distortions toward octahedral geometry, but

TABLE V
ATOMIC PARAMETERS AND ANISOTROPIC TEMPERATURE FACTORS FOR THE STRUCTURE $[Fe^{II}(py_3TPN)](ClO_4)_2$

Atomic Parameters

Atom	*x*	*y*	*z*	*B*
Fe	0.1828 (2)	0.1737 (1)	0.2052 (3)	*a*
Cl(1)	0.3568 (5)	0.0820 (2)	−0.2904 (6)	*a*
Cl(2)	0.2646 (5)	0.4021 (3)	−0.4916 (7)	*a*
O(11)	0.346 (2)	0.147 (1)	−0.278 (2)	*a*
O(12)	0.460 (1)	0.064 (1)	−0.273 (2)	*a*
O(13)	0.355 (2)	0.070 (1)	−0.420 (2)	*a*
O(14)	0.269 (2)	0.050 (1)	−0.233 (2)	*a*
O(21)	0.149 (1)	0.391 (1)	−0.504 (2)	*a*
O(22)	0.318 (2)	0.387 (1)	−0.604 (2)	*a*
O(23)	0.293 (2)	0.462 (1)	−0.459 (2)	*a*
O(24)	0.310 (2)	0.359 (1)	−0.401 (2)	*a*
N(1)	0.102 (1)	0.122 (1)	0.319 (2)	*a*
N(2)	0.074 (1)	0.134 (1)	0.084 (1)	*a*
N(3)	0.284 (1)	0.190 (1)	0.343 (1)	*a*
N(4)	0.302 (1)	0.111 (1)	0.162 (1)	*a*
N(5)	0.096 (1)	0.243 (1)	0.264 (1)	*a*
N(6)	0.229 (1)	0.239 (1)	0.080 (2)	*a*
C(1)	0.093 (2)	0.219 (1)	0.617 (2)	3.8 (4)
C(2)	0.126 (2)	0.204 (1)	0.479 (2)	3.5 (4)
C(3)	0.106 (2)	0.133 (1)	0.455 (2)	2.4 (4)
C(4)	0.028 (2)	0.085 (1)	0.275 (2)	2.8 (4)
C(5)	0.012 (2)	0.087 (1)	0.140 (2)	2.8 (4)
C(6)	−0.060 (2)	0.049 (1)	0.071 (2)	3.1 (4)
C(7)	−0.074 (2)	0.061 (1)	−0.056 (2)	4.1 (5)
C(8)	−0.016 (2)	0.109 (1)	−0.113 (2)	4.5 (5)
C(9)	0.056 (2)	0.146 (1)	−0.036 (2)	4.0 (5)
C(10)	0.246 (2)	0.222 (1)	0.452 (2)	3.2 (4)
C(11)	0.373 (2)	0.155 (1)	0.347 (2)	2.9 (4)
C(12)	0.389 (2)	0.111 (1)	0.242 (2)	3.8 (4)
C(13)	0.482 (2)	0.074 (1)	0.231 (2)	4.8 (5)
C(14)	0.485 (2)	0.032 (1)	0.132 (2)	4.7 (5)
C(15)	0.399 (2)	0.032 (1)	0.047 (2)	4.2 (5)
C(16)	0.307 (2)	0.070 (1)	0.066 (2)	3.9 (4)
C(17)	0.043 (2)	0.242 (1)	0.388 (2)	2.6 (4)
C(18)	0.102 (2)	0.295 (1)	0.206 (2)	3.0 (3)
C(19)	0.174 (2)	0.292 (1)	0.094 (2)	2.6 (3)
C(20)	0.178 (2)	0.341 (1)	0.003 (2)	4.3 (4)
C(21)	0.244 (2)	0.332 (1)	−0.100 (2)	5.8 (6)
C(22)	0.307 (2)	0.287 (1)	−0.113 (2)	4.8 (5)
C(23)	0.295 (2)	0.232 (1)	−0.019 (2)	3.1 (4)

Anisotropic Temperature Factors ($\times 10^4$)

Atom	β_{11}	β_{22}	β_{33}	β_{12}	β_{13}	β_{23}
Fe	54 (2)	11	59 (2)	−1 (1)	4 (2)	−4 (1)
Cl(1)	90 (7)	25 (2)	104 (8)	−3 (3)	−7 (8)	0 (4)
Cl(2)	65 (8)	16 (3)	164 (9)	2 (3)	4 (8)	1 (5)
O(1)	288 (13)	27 (8)	381 (22)	42 (7)	−171 (13)	−23 (10)
O(2)	138 (12)	34 (7)	163 (18)	15 (6)	−65 (12)	2 (8)
O(3)	164 (17)	60 (8)	100 (12)	18 (7)	12 (13)	2 (9)
O(4)	158 (16)	128 (9)	120 (18)	−82 (10)	31 (14)	−28 (11)
O(5)	57 (13)	48 (10)	275 (16)	−1 (11)	−33 (10)	−19 (15)
O(6)	287 (18)	78 (11)	233 (14)	−19 (8)	187 (11)	−26 (13)
O(7)	126 (13)	28 (14)	392 (21)	19 (9)	−6 (10)	11 (12)
O(8)	158 (18)	31 (8)	186 (12)	6 (8)	−81 (13)	4 (11)
N(1)	53 (14)	4 (3)	102 (2)	5 (5)	−9 (13)	−42 (7)
N(2)	37 (14)	13 (4)	54 (15)	−2 (6)	−14 (11)	−3 (6)
N(3)	28 (13)	11 (3)	64 (14)	−13 (5)	4 (10)	2 (6)
N(4)	50 (13)	9 (3)	58 (13)	4 (6)	4 (12)	5 (6)
N(5)	42 (13)	19 (3)	41 (14)	5 (5)	−2 (10)	7 (6)
N(6)	37 (13)	18 (4)	95 (18)	9 (6)	15 (13)	2 (8)

[a] See anisotropic temperature factors.

the effect is much more pronounced for the latter.

In order to attempt to rationalize these findings, several factors affecting the overall energy of the complex ion should be considered, notably (a) the strain energy of the ligand, (b) interligand atom repulsion energy, and (c) ligand-field stabilization energies. Since these structures are determined in the solid state, crystal packing energies and intermolecular forces may contribute to the overall geometry of the ions but are probably small in relation to these other effects.

Consideration of interligand atom repulsion forces[19] predicts the most stable geometry for the coordination number six to be an octahedral arrangement, and it is only by virtue of the special steric requirements of the ligands of Table VI that nonoctahedral structures are observed for these complexes. Thus, coordination of the three aldimino nitrogens of PccBF$^-$, py_3tach, and py_3TPN will align the three pyridine nitrogens in a

(19) R. J. Gillespie, *Can. J. Chem.*, **38**, 818 (1960); R. J. Gillespie, *Angew. Chem., Int. Ed. Engl.*, **6**, 819 (1967).

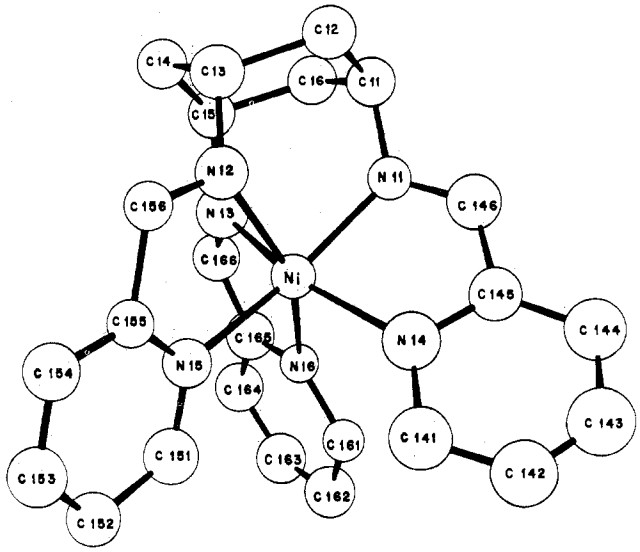

Figure 4.—Structure of one of the two crystallographically independent cations in *cis,cis*-1,3,5-tris(pyridine-2-aldimino)-cyclohexanenickel(II) perchlorate.

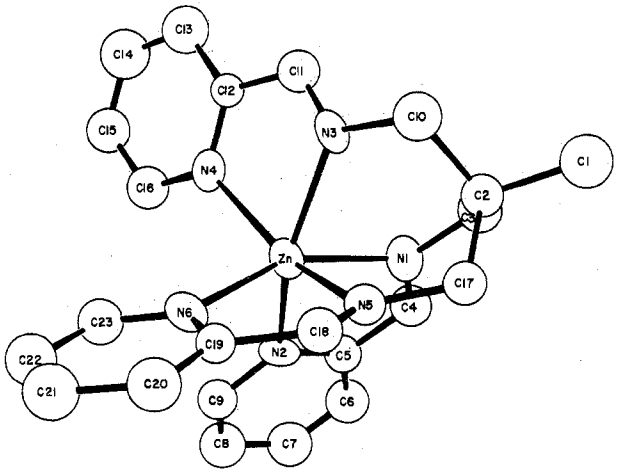

Figure 5—Structure of the cation in 1,1,1-tris(pyridine-2-aldiminomethyl)ethanezinc(II) perchlorate.

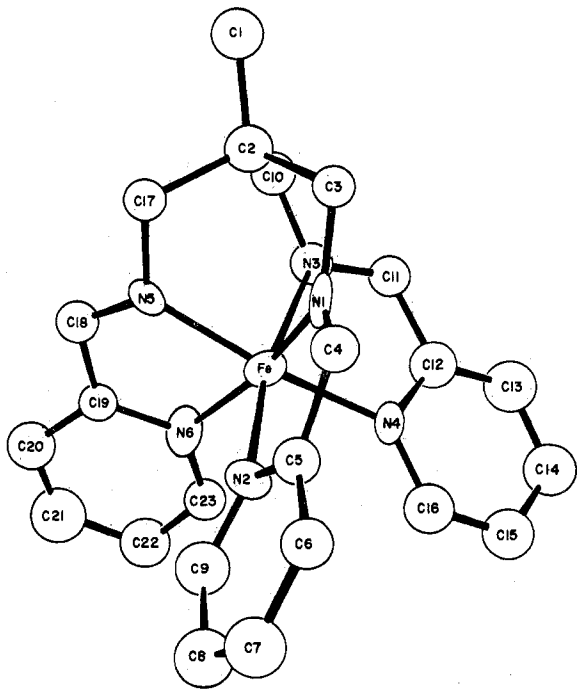

Figure 7.—Structure of the 1,1,1-tris(pyridine-2-aldiminomethyl)-ethaneiron(II) cation.

absence of ligand-field stabilization energies for the two zinc complexes, the resulting structures represent the closest approach to trigonal prismatic coordination allowed by the combination of interligand atom repulsion and ligand strain energies.

Ligand-field stabilization energies are greater for octahedral than trigonal prismatic fields and it has been suggested that this represents a driving force away from trigonal prismatic geometry which is predicted[9] to follow the order (low spin) Fe(II) > Ni(II) > (high spin) Co(II) > (high spin) Mn(II) $\simeq$ Zn(II). Both this and the interligand repulsion term can only favor distortions of the geometry toward an octahedron at the expense of a strain energy in the ligand. Thus the extra rigidity of the cyclohexane "capping group" of

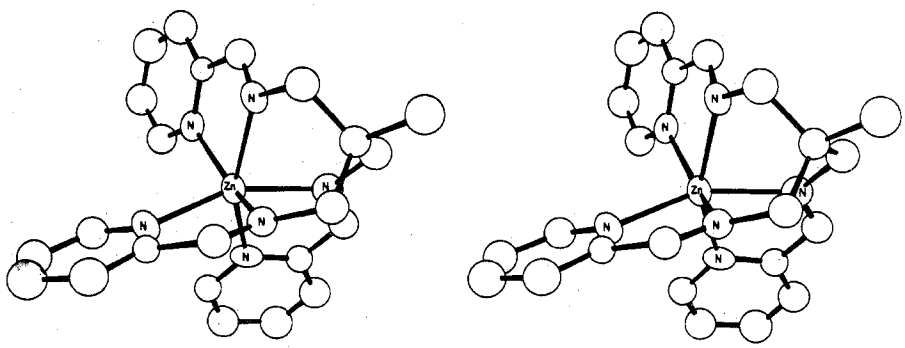

Figure 6.—A stereodiagram of the cation, $Zn(py_3TPN)^{2+}$.

trigonal prismatic manner by virtue of the planar pyridine-2-carboxaldimino chelate arms. In this way the ligand would have a strain-free conformation apart from a steric crowding of the hydrogen atoms attached to the carbon-6 atoms of the pyridine rings in the ligands of the open trifurcated type (py_3tach and py_3TPN). This steric crowding is absent in the bicyclic ligands $PccBF^-$ and $(dmg)_3(BF)_2^{2-}$. In the py_3tach is reflected in the much smaller $\bar{\phi}$ for $Zn(py_3tach)^{2+}$ than for $Zn(py_3TPN)^{2+}$, since the latter can be distorted more easily to allow a more favorable interligand atom repulsion term. It is of interest to note that although increasing $\bar{\phi}$ produces a strain in the bonds of the ligands it may also decrease the steric crowding of the carbon-6 hydrogen atoms of the pyridine rings (*vide supra*). This crowding causes[9]

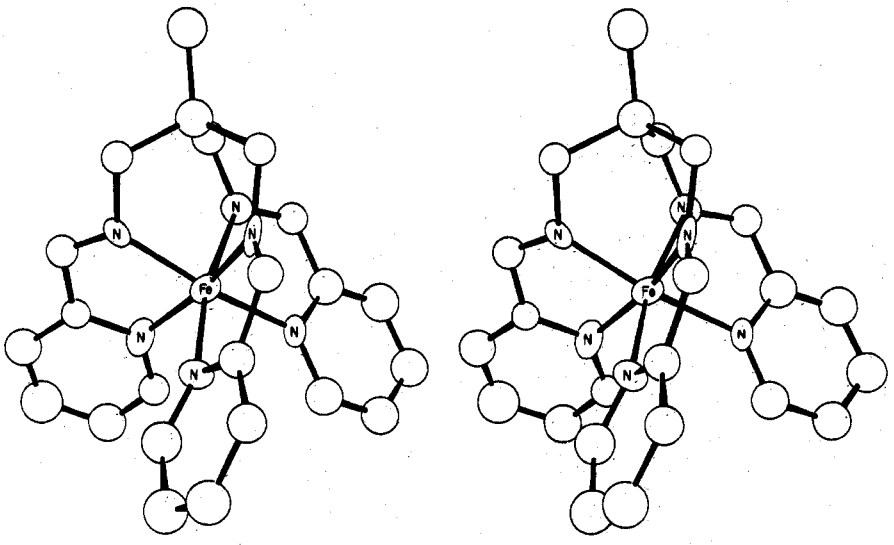

Figure 8.—Stereodiagram of the cation, $Fe(py_3TPN)^{2+}$.

TABLE VI

Complex	Av ϕ, deg	Ref
$Zn(py_3tach)^{2+}$	4.6	9
$Ni(py_3tach)^{2+}$	32	*a*
$Zn(py_3TPN)^{2+}$	28	*a*
$Fe(py_3TPN)^{2+}$	43	*a*
$Ni(PccBF)^{+}$	1.6	7
$Fe(PccBF)^{+}$	21	7
$Co(dmg)_3(BF)_2$	8.6	8
$Co(dmg)_3(FB)_2^{+}$	31.2	8
$Fe(py_3tren)^{2+}$	54	12

[a] This work.

the "opening up" of the triangle of pyridine nitrogen atoms in $Zn(py_3tach)^{2+}$, and consequently longer $Zn-N_{py}$ distances (mean 2.25 Å) are observed than those in the more octahedral complex $Zn(py_3TPN)^{2+}$ (mean 2.16 Å). The mean zinc–aldimino nitrogen bond length is the same for both complexes (2.15 Å).

Increased importance of the ligand-field stabilization energy terms probably accounts for the greater "twist" toward octahedral geometry when comparing $Fe(py_3TPN)^{2+}$ with $Zn(py_3TPN)^{2+}$, $Ni(py_3tach)^{2+}$ with $Zn(py_3tach)^{2+}$, $Fe(PccBF)^{+}$ with $Ni(PccBF)^{+}$, and $Co(dmg)_3(BF)_2^{+}$ with $Co(dmg)_3(BF)_2$. The relative sizes of $\bar{\phi}$ for these pairs of compounds follow the predictions[9] of Wentworth, *et al.*

Indications of a twist toward octahedral geometry are provided[1] by the examination of the methylene proton signals in the nmr spectrum of the Fe(II) complex of py_3TPN. The equivalence of the two methylene protons in a trigonal prismatic form of the ligand is removed as the six ligand atoms are twisted toward an octahedron. The greater separation of the signals of the two protons in $Fe(py_3TPN)^{2+}$ (τ 6.12 and 6.08) when compared with $Zn(py_3TPN)^{2+}$ (τ 5.93 and 5.92) was thought[1] to parallel the greater angle of "twist" found for the Fe(II) complex. However recent studies[20] have shown the irradiation at the azomethine proton resonance position results in collapse of the methylene doublet of $Zn(py_3TPN)^{2+}$ and suggest that in this case the splitting of the methylene signal results from coupling between the methylene protons and the azomethine proton. Even in cases where it can be established that splitting of the methylene signal is due to magnetic nonequivalence of the protons a quantitative relationship between the observed splitting and $\bar{\phi}$ is not possible without a knowledge of the shielding effects of the metal ions on the ligand resonances. It is not valid to assume that complexes showing a singlet for the methylene signal exist in a trigonal prismatic form in solution, because a rapid racemization of pseudooctahedral forms could average the environments of the two methylene protons.

In a recent study,[20] the temperature dependence of the coalescence of the methylene signals of $Fe(py_3TPN)^{2+}$ was used to study the rate of racemization of the assumed pseudooctahedral complex. The activation parameters ($\Delta H^{\ddagger}$ = 18.4 kcal mol^{-1} and $\Delta S^{\ddagger}$ = 1.0 cal deg^{-1} mol^{-1}) are significantly lower than those reported[21] for the racemization of tris(*o*-phenanthroline)iron(II). In both cases a twist mechanism involving trigonal prismatic coordination is thought[20,21] to be involved. It is likely that the lower enthalpy of activation for $Fe(py_3TPN)^{2+}$ results from a reduction in strain energy of the ligand during the twisting process. A knowledge of the factors determining the stability of trigonal prismatic geometry relative to that of octahedral is clearly important in predicting rates of racemization of pseudooctahedral tris chelates *via* a trigonal twist mechanism.

Visible spectroscopy of solutions of the complexes might be hoped to provide information on the geometry of the ligand atoms. Despite the large twist parameter $\bar{\phi}$, the complex $Ni(py_3tach)^{2+}$ shows bands[9] in the solid state (λ_{max} = 11,100, 12,100, and 19,400 cm^{-1}) in remarkably similar positions to those observed for typical octahedral high-spin nickel(II) complexes with similar donors, *e.g.*, $Ni(bipy)_3^{2+}$ (λ_{max} 11,400–11,690, 12,660–12,740, and 18,870–19,600 cm^{-1}).[22] However, in solution the extinction coefficients for these bands for $Ni(py_3TPN)^{2+}$ (ϵ 21, 28, and 69) and for $Ni(py_3tach)^{2+}$ (ϵ 25, 25, and 40)[9] are larger than those for $Ni(bipy)_3^{2+}$ (ϵ 5.7, 7.1, and 11.6).[22] Anomalously high values for the Racah parameter B ($Ni(py_3TPN)^{2+}$,

(20) F. L. Urbach and S. O. Wandiga, *Chem. Commun.*, 1572 (1970); S. O. Wandiga, J. E. Sarneski, and F. L. Urbach, *Inorg. Chem.*, **11**, 1349 (1972).

(21) F. Basolo, J. C. Hayes, and H. M. Neumann, *J. Amer. Chem. Soc.*, **76**, 3807 (1954).

(22) R. A. Palmer and T. S. Piper, *Inorg. Chem.*, **5**, 864 (1966).

TABLE VII
ELECTRONIC ABSORPTION SPECTRA, EFFECTIVE MAGNETIC MOMENTS, AND CARBOXALDIMINO (C=N) STRETCHING FREQUENCIES

Complex	λ, cm^{-1}	ε	μ_{eff}, BM[a,b]	ν(C=N), cm^{-1}
$[Fe(py_3TPN)](ClO_4)_2$	15,000	11,000	0.93	<1610
	19,000 (sh)	7,000		
	28,200	3,200		
	35,000 (sh)	18,000		
	36,400	22,000		
	42,500 (sh)	17,000		
$[Zn(py_3TPN)](ClO_4)_2$			Diamag	1673 (sh), 1663
$[Co(py_3TPN)](ClO_4)_2$	11,500 (sh)	33	4.66	1660 (sh), 1651
	19,100 (sh)	224		
	21,500 (sh)	302		
	29,000	2,320		
	36,400	20,300		
	43,500 (sh)	27,100		
$[Mn(py_3TPN)](ClO_4)_2$			5.85	1656 (sh), 1648
$[Ni(py_3TPN)](ClO_4)_2$	11,200 (br)	21	3.04	1660 (sh), 1650
	12,400 (br)	28		
	20,000 (sh)	69		
	27,000 (sh)	412		
	35,800	46,400		
	41,600	30,200		

[a] Analyses performed by Micro-Tech Laboratories, Inc., Skokie, Ill. [b] After correction for ligand diamagnetism; T = 295°K; (sh) = shoulder and (br) = broad.

B = 1000 cm^{-1} and $Ni(py_3tach)^{2+}$, B = 980 cm^{-1}) are obtained from an interpretation of the spectra on the basis of an octahedral model (*cf.*, $Ni(bipy)_3^{2+}$, B = 750 cm^{-1}). Energy levels calculated for a regular trigonal prismatic model have been used[9] with some success in interpreting the spectrum of $Ni(py_3tach)^{2+}$, but any attempts at evaluation of $\bar{\phi}$ from such spectra will have to await further studies.[23]

The other complex absorbing in the visible region whose structure was determined in this work is $Fe(py_3TPN)^{2+}$. Like $Fe(py_3tach)^{2+}$ this shows strong charge-transfer bands similar to those observed in $Fe(bipy)_3^{2+}$. However, since it is known[24] that the band positions in octahedral tris(α-diimine)iron(II) complexes are very sensitive to the nature of the ligand system, it is unlikely that these will prove useful in detecting changes in $\bar{\phi}$ for the different ligands of Table VI.

It might be anticipated that distortion of the ligand away from its preferred conformation would be accompanied by clearly defined changes in the vibrational spectra of specific functional groups, and that these shifts could be used to monitor the extent of the distortion. The carboxaldimino C=N stretching frequencies are observed to vary with the nature of M^{2+} in the py_3TPN complexes (see Table VII), but as in the $M(py_3tach)^{2+}$ series[9] it is not clear to what extent these changes are due to the distortion causing rotation in the C=N bond or to small changes in the bond order or bond strength due to dependence on the nature of bonding to M^{2+}; it is of interest to note that this frequency appears split for py_3TPN complexes. The large difference in $\bar{\phi}$ for the Ni(II) and Zn(II) complexes of py_3tach is accompanied by a shift of only ≃25 cm^{-1} for the C=N stretching frequency while the Fe(II) complex exhibits a shift of ≃120 cm^{-1} when compared with the Zn(II),[9] making it unlikely that these shifts are due in large part to distortions arising from trigonal twist, but are more likely due to extensive metal to ligand π bonding as evidenced by the charge-transfer bands in the Fe(II) complexes.

The discussion above related only to complexes whose $\bar{\phi}$ values have been determined directly in the solid state. Matching of precession photographs and cell parameters has led to the conclusion that in the $[M(py_3TPN)](ClO_4)_2$ series the Mn(II), Co(II), and Ni(II) complexes are isomorphous with the Zn(II) complex. It is not clear what maximum variation of $\bar{\phi}$ from that found for zinc would be permissible without changing the packing characteristics of the $M(py_3TPN)^{2+}$ ion sufficiently to cause a change of space group or appreciably alter the cell constants. The pairs of compounds in Table VI containing the same ligand, but showing different structures and space groups, have large differences in twist angles $\bar{\phi}$ (py_3tach, 28°; py_3TPN, 15°; PccBF⁻, 19°; and $(dmg)_3(BF)_2^{2-}$, 23°). It is therefore possible that significant variations in twist may exist for an isomorphous series and it would be unwise to assume a constant value of twist in interpreting other physical data. Verification of similarity or significant variation in a pair of isomorphous structures must await an independent structural determination for a second member of one of these series.

Summary

The results of these and other[7-9,12] structure determinations have confirmed a range of coordination geometries for the complexes in Figures 2a, 2b, 3a, 3b, and 3c varying between idealized trigonal prismatic and octahedral forms. The geometry observed can be rationalized on the basis of ligand rigidity favoring trigonal prismatic coordination in the order PccBF⁻ > $(dmg)_3(BF_2)^{2-}$ > py_3tach > py_3TPN > py_3tren and ligand-field stabilization energy favoring octahedral coordination following the order (low spin) Co(III) > (low spin) Fe(II) > Ni(II) > (high spin) Co(II) > (high spin) Mn(II) ≃ Zn(II).

Acknowledgment.—We gratefully acknowledge the support of the National Science Foundation and the National Institutes of Health.

(23) A more detailed study of crystal spectra and nmr spectra has been carried out and may lead to more definitive results: R. H. Holm, personal communication.

(24) P. Krumholtz, *J. Amer. Chem. Soc.*, **75**, 2163 (1953).